

# On the variability of 47Tuc W (to be decided)

Pavan R. Hebbar,<sup>1</sup><sup>★</sup> Craig O. Heinke,<sup>2</sup><sup>†</sup>

<sup>1</sup>*Department of Physics, University of Alberta*

<sup>2</sup>*Department of Physics, University of Alberta*

Accepted XXX. Received YYY; in original form ZZZ

## ABSTRACT

**Key words:** keyword1 – keyword2 – keyword3

## 1 INTRODUCTION

## 2 OBSERVATIONS

Due to the compact core of 47 Tuc, the arc-second resolution of *Chandra X-ray observatory* was used to investigate the 47 Tuc W system. Data from ACIS-S 2002 observations (exposure of  $\sim 300$ ks) and 2014-15 observations (exposure of  $\sim 200$ ks) have been used to analyze the spectrum and the X-ray light curve of the system. HRC observations of 2005-06 (exposure of  $\sim 800$ ks) has been also been used. The details of all the observations used are summarized in Table 1. The new observations of 2014 – 15 have supplemented in the detection of 50 additional sources (Bhattacharya et al., 2017) including the previously undetected X-ray counterparts of the pulsars with known positions.

### 2.1 Data Reduction

CIAO version 4.9 was used for data reduction and image processing. The initial data downloaded from WebChASeR was reprocessed according to CALDB 4.7.6 calibration standards using the `chandra_repro` command. The X-ray photons corresponding to 47 Tuc W system were extracted from a circular region of 1" radius around the source. This region was selected as a compromise between selecting maximum photons from the interested source, and avoiding photons from the neighboring sources. Photons were corrected for barycentric shifts using the `axbary` tool of CIAO to remove the effect of earth's motion around sun. The aspect solution file and the exposure statistics file were also corrected in order to correct the good time intervals. These barycenter corrected files were used for further analysis. 5 regions close to the 47 Tuc W system were chosen for the background subtraction and barycentric correction applied on them to take the variability of background into account.

### 2.2 Variability analysis

The ephemeris data of 47 Tuc W system from Ridolfi et. al. 2016 was used to prepare the phase folded light curve. Given that the orbital frequency  $f = 8.71 \times 10^{-5}$  and  $\Delta f/f \sim 10^{-5}$ , the change in the orbital frequency was neglected. A reference epoch of 51585.3327 MJD was used (time of passage of perigee). Phase folded light curves were constructed separately for each observations from the corresponding barycenter corrected source and background files using `dmtcalc` and `dmextract` commands. The light curves corresponding to the 2002 observations, 2004-05 observations and 2014-15 observations were added separately. This was done to increase the number of data points and to look into any possible differences in the light curves across the three observations. Gehrels formulation (Gehrels 1986) was used to calculate the error in the source photons and gaussian error was used for background photons. In order to study the variability across different energy bands. Additional light curves were made for very low energy band (0.2 - 1.0 keV), low energy band (0.3 - 2.0 keV) and high energy band (2.0 - 8.0 keV) for the 2002 and 2014-15 observations to further study the system.

### 2.3 Spectral analysis

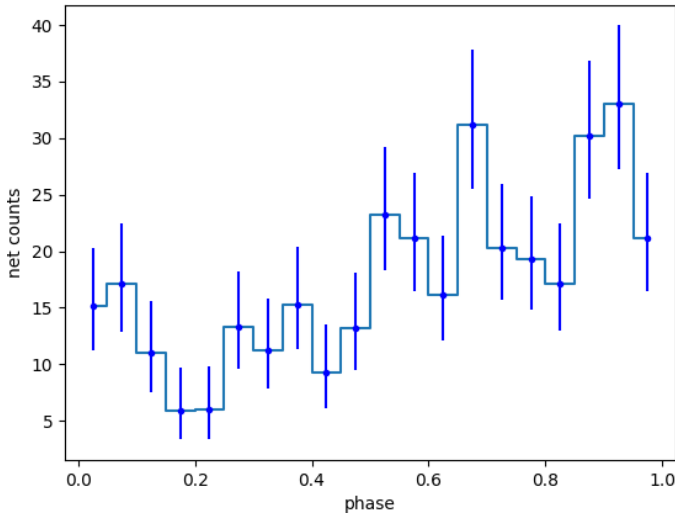
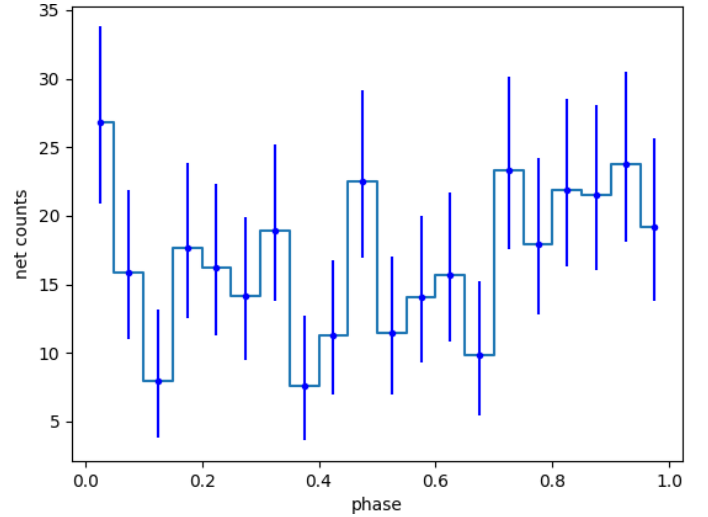
The HRC observations do not contain any information regarding the energy of the photons and hence cannot be used for spectral analysis. Data from 2002 and 2014-15 observations were analyzed separately to investigate any change in the spectrum. To look into the nature of the transits, the data from the intervals when the 47 Tuc W system was in transit was grouped separately from the intervals when the system was not in transit. For this purpose, good time intervals corresponding to the required phases, were extracted from the `dmgti` tool and aligned to the corresponding ACIS observations using `gti_align` tool. The spectrum from individual observations were then extracted from `spec_extract` tool and then combined using `combine_spectra` in order to increase the photon count. In order to reduce the error bars, the spectra were then grouped so that each energy bin contained a specific number of photons. This number was 8 for the spectrum from transit time intervals and 15 for the spectrum from remaining times.

<sup>★</sup> E-mail: hebbar@ualberta.ca

<sup>†</sup> E-mail: heinke@ualberta.ca

**Table 1.** Summary of X-ray observations used

Obs ID	Instrument	Exposure(ks)	Start Date	Obs ID	Instrument	Exposure(ks)	Start Date
2735	ACIS-S	65.24	2002-09-29 16:57:56	5542	HRC-S	49.76	2005-12-19 07:03:06
3384	ACIS-S	5.31	2002-09-30 11:37:18	5543	HRC-S	50.65	2005-12-20 14:57:42
2736	ACIS-S	65.24	2002-09-30 13:24:28	5544	HRC-S	49.83	2005-12-21 23:25:20
3385	ACIS-S	5.31	2002-10-01 08:12:28	5545	HRC-S	51.64	2005-12-23 05:01:54
2737	ACIS-S	65.24	2002-10-02 18:50:07	5546	HRC-S	48.27	2005-12-27 05:33:43
3386	ACIS-S	5.54	2002-10-03 13:37:18	6230	HRC-S	44.77	2005-12-28 13:44:36
2738	ACIS-S	68.77	2002-10-11 01:41:55	6231	HRC-S	46.89	2005-12-29 21:50:23
3387	ACIS-S	5.73	2002-10-11 21:22:09	6232	HRC-S	44.15	2005-12-31 05:17:20
15747	ACIS-S	50.04	2014-09-09 19:32:57	6233	HRC-S	97.18	2006-01-02 05:37:31
15748	ACIS-S	16.24	2014-10-02 06:17:00	6235	HRC-S	49.93	2006-01-04 04:04:57
16527	ACIS-S	40.88	2014-09-05 04:38:37	6236	HRC-S	51.7	2006-01-05 11:29:07
16528	ACIS-S	40.28	2015-02-02 14:23:34	6237	HRC-S	49.96	2005-12-24 14:07:36
16529	ACIS-S	24.7	2014-09-21 07:55:51	6238	HRC-S	48.2	2005-12-25 21:12:00
17420	ACIS-S	9.13	2014-09-30 22:56:03	6239	HRC-S	49.88	2006-01-06 22:08:49
				6240	HRC-S	49.07	2006-01-08 02:19:31

**Figure 1.** Phase folded light curve of 47 Tuc W from 2002 observations after background subtraction. Light curves have been folded with a period of 11486.4 seconds and a reference epoch of 51585.3327 MJD. Errors have been calculated using gehrels formulation. Transit can clearly be seen in the light curve from 0.1 - 0.4 phase**Figure 2.** Phase folded light curve of 47 Tuc W from 2005 observations after background subtraction. This light curve is significantly different from the one from 2002 observations. Though the light curve does show some features, they are within the error limits and are not of statistical importance.

## 2.4 X-ray Variability

Light curves from 2002 ACIS observations and 2004-05 HRC observation were extracted again, after accounting for the changes in the calibration standards. Figure 1 shows the phase folded light curve from the 2002 observations. Dips in the light curve can be seen as pointed by Bogdonov et al. 2005. In order to confirm the nature of these transits, the data was fit to a constant and  $\chi^2_\nu$  was calculated. A  $\chi^2_\nu$  value of 2.156 proves the existence of the transit. Figure 2 is phase folded light curve from the 2004-05 observations. As can be seen from the graph the dip's in the light curve are less prominent. Fitting this curve to a constant value gives  $\chi^2_\nu = 0.822$ , thus proving the statistical insignificance of the changes in the light curve.

Figure 3 shows the light curve extracted from the 2014 - 15 ACIS observations. Note that the light curve is very similar to that from 2002 observations. Periodic transit in the light curve

can be observed in this light curve too. The position of these dips match exactly (both reach minimum at phase 0.2). Given that the 2002 observations have about 1.5 times the exposure of 2014 - 15 observations, even the photon count rate is similar within the error limits. A constant fit to the light curve gives  $\chi^2_\nu = 2.062$  - slightly reduced because of increased errors (due to less photon counts). This indicates that the 47 Tuc W system hasn't evolved in these 12 years.

To explain the difference in the 2005 light curve from the other two light curves and investigate the gross properties of the 47 Tuc W system, a scatter plot of photon energy v/s phase was plotted for all events as shown in figure 4. The density of points in a region depict the number of photons observed with the given energy during a given phase. From the figure, it can be seen that the dips in the number of photons are much more prominent for high energy photons as compared to the lower energy photons which shows almost no decrease in the number. Thus the higher sensitivity of HRC photons to lower energy x-rays might be the reason for the

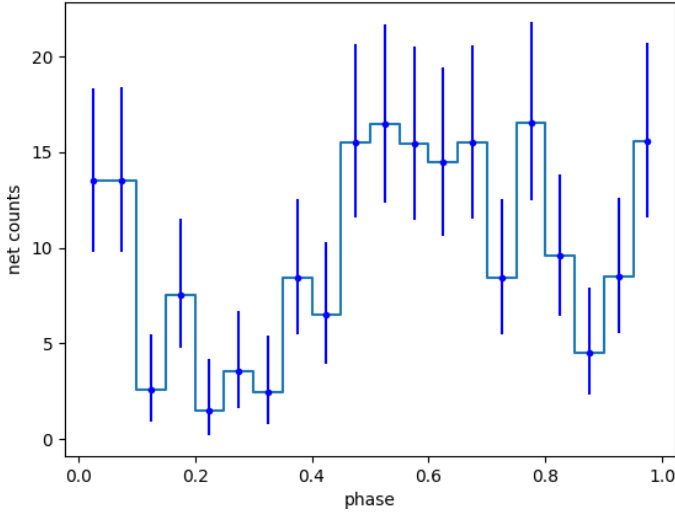


**Figure 3.** Phase folded light curves from 2014-15 observations. The features and the count rate is very similar to the 2002 observations

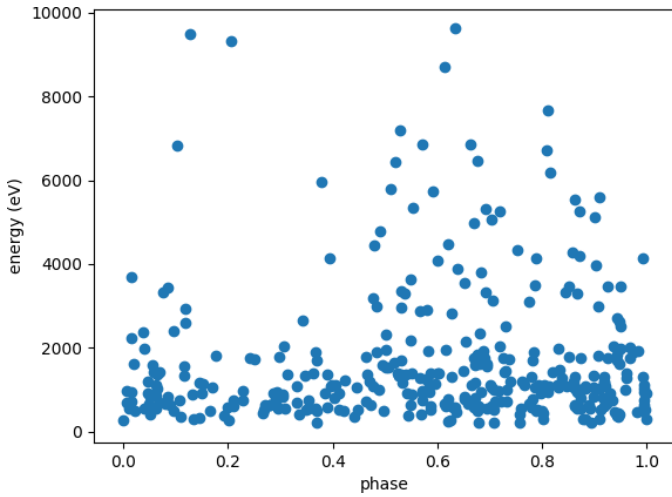


**Figure 4.** Scatter plot of photon energy v/s phase. While the density of the points stays roughly constant in the lower energy, it shows significant changes for the higher energies

absence of transits. To investigate this, light curve was plotted for the 2002 observations for photons between 0.3 - 2.0 keV as shown in figure 5. A constant fit to this light curve gives  $\chi^2_{\nu} = 1.173$ . So the light curve was further restricted to energy interval 0.2 - 1.0 keV and plotted in figure 5. In this case the  $\chi^2_{\nu}$  was further reduced to 0.699. Also this plot looks similar to the light curve from HRC data implying that the differences in the light curves of ACIS and HRC observations could be due to observational bias because of the difference in the sensitivity of the two detectors. On the other hand, in figure 6 - the light curve for high energy photons (3.0 - 8.0 keV) from the ACIS 2002 observations, the change in the light curve is much more significant.

Figure 7 show the light curves of low energy, very low energy and high energy photons for 2014-15 observations. The similarity in the light curves of 2002 and 2014-15 observations increases the confidence in the hypothesis that observational bias is the reason why the light curves of 2005-06 observations are different.

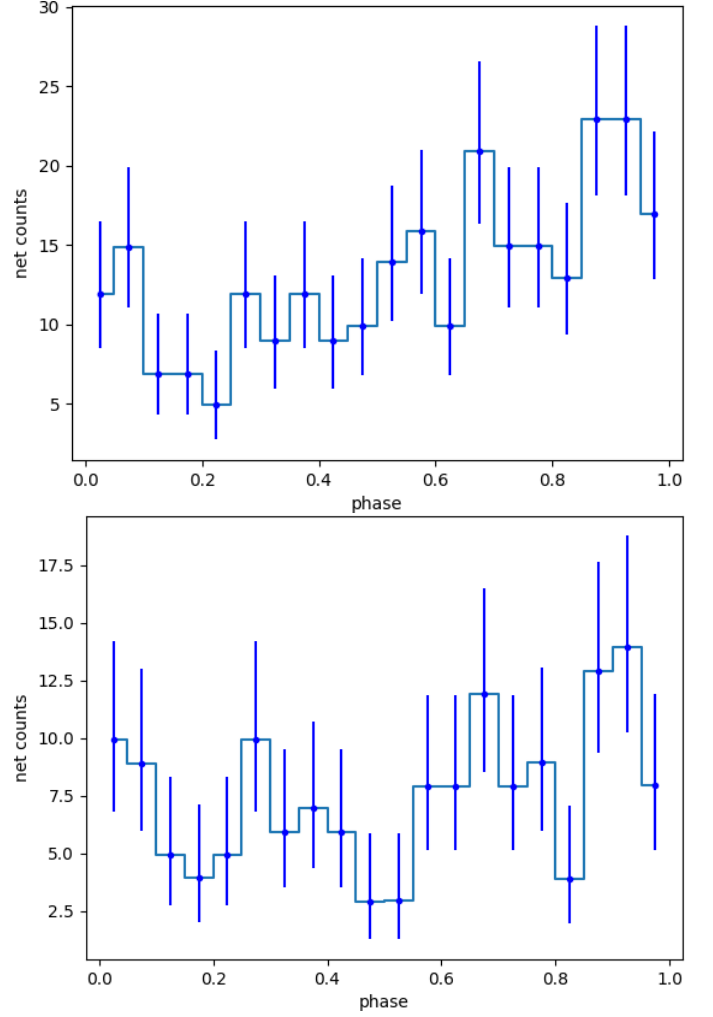


**Figure 5.** Phase folded light curves for (top) 0.3 - 2.0 keV photons and (bottom) 0.2 - 1.0 keV photons from ACIS 2002 observations. The dips in the light curve are less significant for lower energies

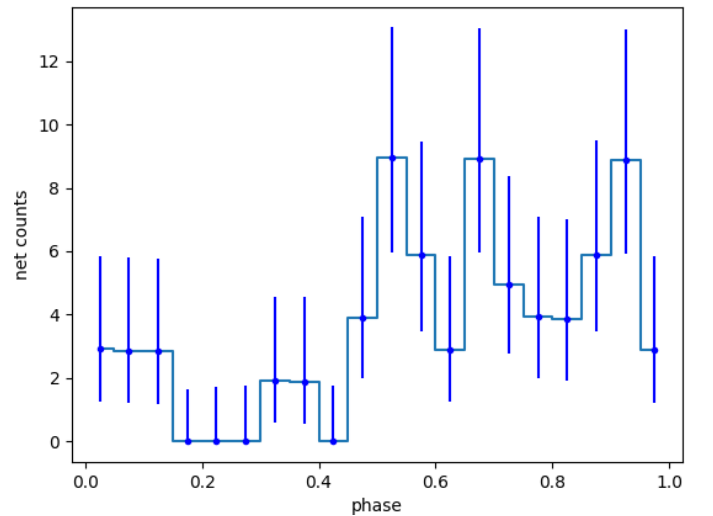


**Figure 6.** Light curve for 2.0 - 8.0 keV.  $\chi^2_{\nu} = 1.171$  for a constant fit.  $\chi^2_{\nu}u$  is low due to less photon count ( $\approx 73$ ) as compared to low energy ( $\approx 260$ )

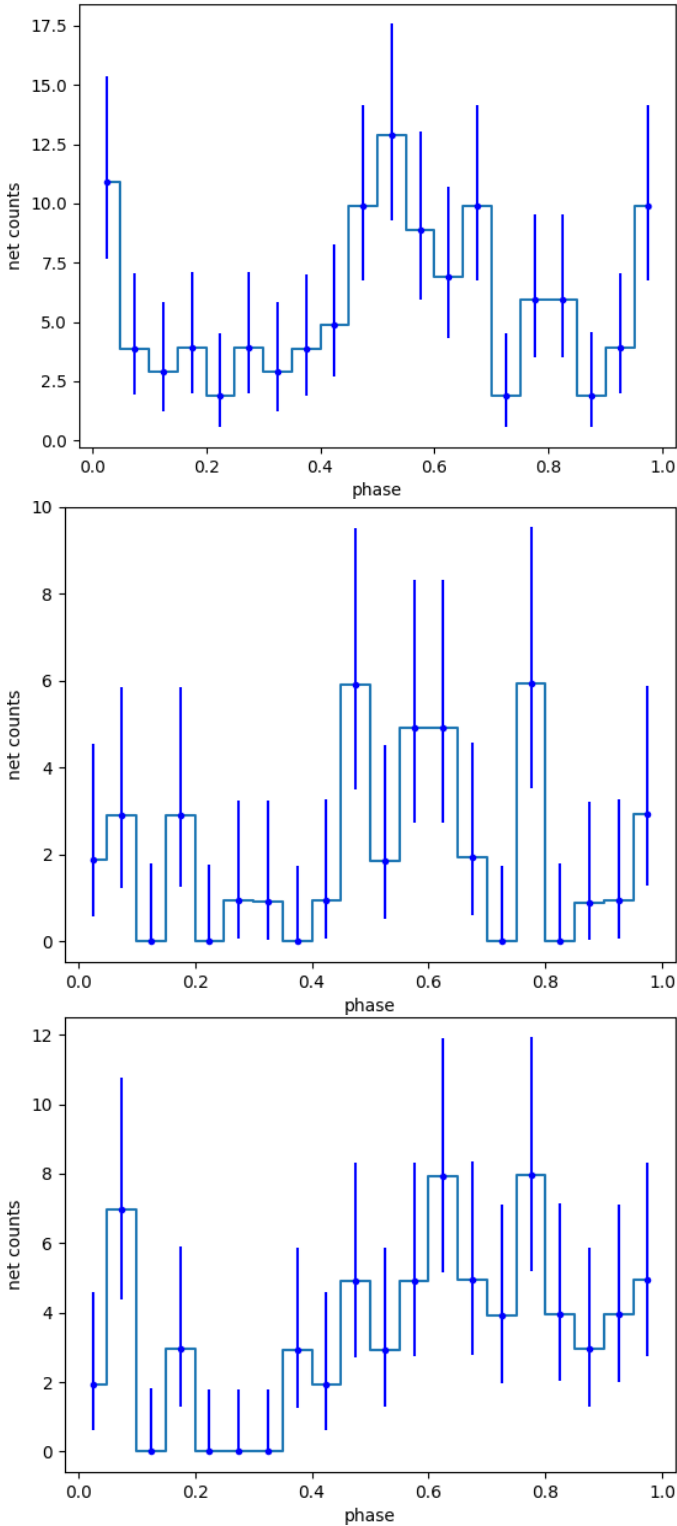


**Figure 7.** Phase folded light curves for different energy bands for 2014-15 observations. (top) low energy photons.  $\chi^2_\nu = 0.875$  for a constant fit. (middle) very low energy photons.  $\chi^2_\nu = 0.581$  for a constant fit. (bottom) high energy photons.  $\chi^2_\nu = 0.977$  for a constant fit (low value because of  $\approx 70$  counts leading to large error bars). Note that all the  $\chi^2_\nu$  values are low than their corresponding values in 2003 observations due to the less exposure time in 2014-15 observations leading to low photon counts and larger error.

### 3 X-RAY SPECTRUM

The X-ray spectrum for 47 Tuc W system was analysed for 0.3 - 10.0 keV photons where ACIS instrument has highest sensitivity. Data was divided into 4 groups to look into any changes in the spectra during transits and between the 2002 and 2014-15 observations:

- **D1** - Data from 2002 observations extracted from phases where there is no transit (phases 0.0-0.1 and 0.4- 1.0)
- **D2** - Data from 2014-15 observations extracted from phases where there is no transit (phases 0.0-0.1 and 0.4-1.0)
- **D3** - Data from 2002 observations when transit is observed (phases 0.1-0.4)
- **D4** - Data from 2002 observations when transit is observed (phases 0.1-0.4)

Due to the low photon counts, the data is assumed to have a Poisson distribution. Thus C-statistic were used to evaluate the results. Also gehrels weights were applied to give better results. The hydrogen column density towards 47 Tuc was taken to be  $3.5 \times 10^{20} \text{ cm}^{-2}$  (Barahmain et al.). The absorptions due to dust was modeled by `tbabs` tool in XSPEC. Due to less data points several approximations had to be made. These models and the reasoning behind these approximations have been described below.

On plotting the data, a power law trend was observed. So all the four data groups were independently fit with a pegged power law with 0.2 keV and 10.0 keV as the energy cutoffs. (model 1). Due to the low photon count the parameters of the spectral fit of D3 and D4 had huge errors. It was observed that the photon indices of D1 and D2 were similar within  $1 \sigma$  error bar, and same could be observed for D3 and D4. So the photon indices of (D1, D2) and (D3, D4) were linked to be same. Fitting a pegged power law, with linked photon indices (model 2) gave  $\Gamma = 1.57 \pm 0.08$  for D1 and D2 and  $\Gamma = 2.62 \pm 0.33$ . Thus it can be concluded that the spectrum becomes soft during the transit indicating the the emission is from two different sources.

The pegged power law fit doesn't explain the spectrum at lower energies. Thus the softer spectrum could be due to emission from the neutron star which could be explained by a Blackbody (BB) (model 3) or a neutron star atmosphere model. From the parameters of the binary orbit of (47 Tuc W) system, it can be calculated the the neutron star is expected to be occulted for 2-5% of the orbit. Since our bins correspond to a larger time interval, the emission from the neutron star can be assumed constant across all phase bins. Thus the parameters of the softer spectrum are assumed to be same across all the data groups. With these approximations a blackbody spectrum could be fit with reasonable magnitude of the errors.

The neutron star atmosphere model was fit using the `nsatmos` model of XSPEC. The neutron star mass was assumed to be 1.44 solar masses and the distance to 47 Tuc W was fixed to 4.85 pc. Since even with these approximations the error in the parameters were large, radius of neutron star was constrained to 20 km. Since `norm` is the fractional part of the neutron star emitting, higher value of radius was chosen and the effective value of radius was calculated. With these approximations the model could be fit with reasonable errors (model 4).

All data have been summarized in Table 2. A plot of the the various elements of model 3 along with the data is shown in figure 8. Figure 8 also shows the various components of models 4.

The black body model for the thermal component gives a total unabsorbed flux of  $6.36 \times 10^{-15} \text{ ergs cm}^{-2} \text{ s}^{-1}$  during the transit and  $1.43 \times 10^{-14} \text{ ergs cm}^{-2} \text{ s}^{-1}$  at other times for the data from 2002 observations. The 2014 - 15 observations seem to give a slightly

Data Groups	Model parameters	Model 1	Model 2	Model 3	Model 4
D1	Power law index	$1.63 \pm 0.10$	$1.58 \pm 0.08$	$1.24 \pm 0.15$	$1.18 \pm 0.16$
	Power law norm	$(1.25 \pm 0.10) \times 10^{-2}$	$(1.30 \pm 0.10) \times 10^{-2}$	$(1.27 \pm 0.12) \times 10^{-2}$	$(1.26 \pm 0.13) \times 10^{-2}$
	Teff	-	-	$(1.65 \pm 0.33) \times 10^6$	$(7.56 \pm 2.26) \times 10^5$
	Radius	-	-	$(2.315.40) \times 10^{-1}$	1.204.63
D2	Power law index	$1.43 \pm 0.15$	$1.58 \pm 0.08$	$1.24 \pm 0.15$	$1.18 \pm 0.16$
	Power law norm	$(1.81 \pm 0.19) \times 10^{-2}$	$(1.73 \pm 0.19) \times 10^{-2}$	$(1.84 \pm 0.20) \times 10^{-2}$	$(1.84 \pm 0.20) \times 10^{-2}$
	Teff	-	-	$(1.65 \pm 0.33) \times 10^6$	$(7.56 \pm 2.26) \times 10^5$
	Radius	-	-	$(2.315.40) \times 10^{-1}$	1.204.63
D3	Power law index	$2.47 \pm 0.34$	$2.61 \pm 0.31$	$1.24 \pm 0.15$	$1.18 \pm 0.16$
	Power law norm	$(5.28 \pm 0.94) \times 10^{-3}$	$(5.45 \pm 1.13) \times 10^{-3}$	$(4.76 \pm 1.42) \times 10^{-3}$	$(4.37 \pm 1.52) \times 10^{-3}$
	Teff	-	-	$(1.65 \pm 0.33) \times 10^6$	$(7.56 \pm 2.26) \times 10^5$
	Radius	-	-	$(2.315.40) \times 10^{-1}$	1.204.63
D4	Power law index	4.047.96	$2.61 \pm 0.31$	$1.24 \pm 0.15$	$1.18 \pm 0.16$
	Power law norm	0.05634.35	$(6.8614.58) \times 10^{-3}$	$(7.94 \pm 2.61) \times 10^{-3}$	$(7.50 \pm 2.72) \times 10^{-3}$
	Teff	-	-	$(1.65 \pm 0.33) \times 10^6$	$(7.56 \pm 2.26) \times 10^5$
	Radius	-	-	$(2.315.40) \times 10^{-1}$	1.204.63
$\chi^2_\nu$ values		0.7922	0.8310	0.7458	0.7168
Unabsorbed flux					

**Table 2.** Parameters of spectral fits in various models for different data groups

larger flux of  $9.5 \times 10^{-15}$  ergs cm $^{-2}$  s $^{-1}$  for the transit intervals and  $2.00 \times 10^{-15}$  ergs cm $^{-2}$  s $^{-1}$  during other times. In both the cases, the reductions in the flux during transits is consistent with that observed in the light curves. The NSA model also gives similar values with two significant digits. In all cases the non thermal flux contributes to  $\approx 75\%$  of the total. The low values of  $\chi^2_\nu$  indicate that more data points are required to reduce the errors and thus get better fits.

#### 4 CONCLUSIONS

The additional data from 2014-15 observations show the existence of the transits in the light curve. Due to less number of photons ( 180 in case of 2014-15 and 300 in case of 2002 data), many of the spectral fitting parameters had to be constrained. More observations are needed to study the properties of the 47 Tuc W system

This paper has been typeset from a  $\text{\LaTeX}$  file prepared by the author.

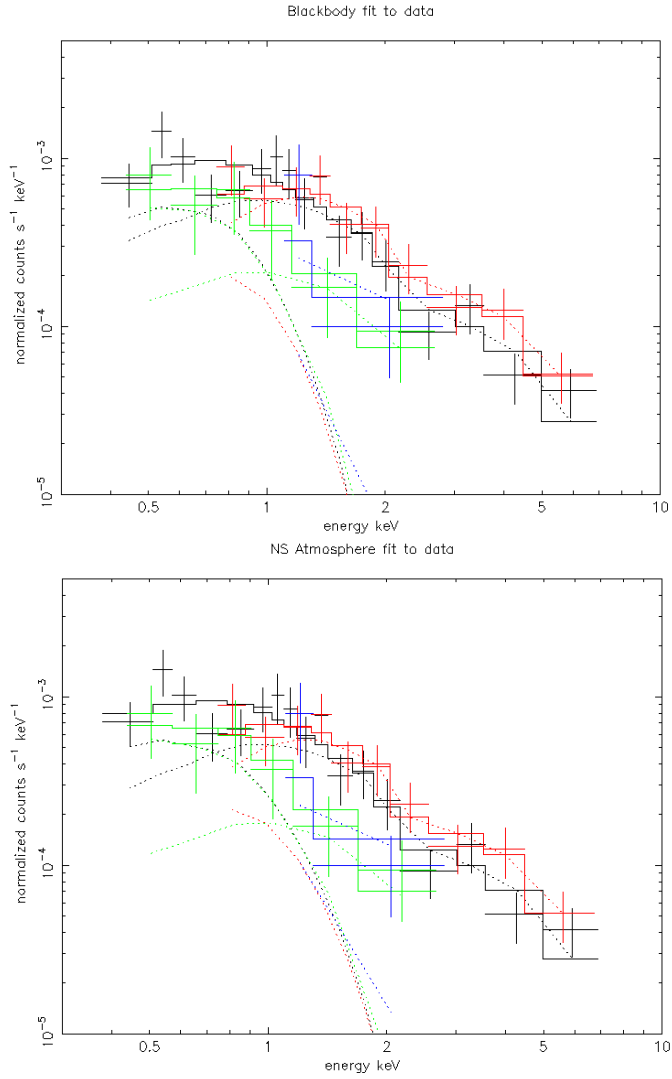


**Figure 8.** Spectral fits to the observed spectrum. (Top) Model with pegged power law and blackbody components with absorption modeled from tbabs. (Bottom) Model with pegged power law and neutron star atmosphere components and absorption modeled from tbabs. Black refers to D1, red refers to D2, green refers to D3 and blue represents D4. The dotted lines represent the corresponding additive components